Error Correlation Between CO2 and CO as Constraint for CO2 Flux Inversions Using Satellite Data

Atmos. Chem. Phys., 9, 7313–7323, 2009
www.atmos-chem-phys.net/9/7313/2009/

Atmospheric Chemistry and Physics

Error correlation between CO_2 and CO as constraint for CO_2 flux inversions using satellite data

H. Wang[1,2], D. J. Jacob[1], M. Kopacz[1], D. B. A. Jones[3], P. Suntharalingam[4], J. A. Fisher[1], R. Nassar[3,5], S. Pawson[6], and J. E. Nielsen[6]

[1]School of Engineering and Applied Sciences, Harvard University, Cambridge, MA, USA
[2]Smithsonian Astrophysical Observatory, Cambridge, MA, USA
[3]Department of Physics, University of Toronto, Toronto, Ontario, Canada
[4]School of Environmental Sciences, University of East Anglia, Norwich, UK
[5]Department of Geography, University of Toronto, Toronto, Ontario, Canada
[6]NASA Goddard Space Flight Center, Global Modeling and Assimilation Office, Greenbelt, MD, USA

Received: 17 February 2009 – Published in Atmos. Chem. Phys. Discuss.: 12 May 2009
Revised: 8 September 2009 – Accepted: 11 September 2009 – Published: 2 October 2009

Abstract. Inverse modeling of CO_2 satellite observations to better quantify carbon surface fluxes requires a chemical transport model (CTM) to relate the fluxes to the observed column concentrations. CTM transport error is a major source of uncertainty. We show that its effect can be reduced by using CO satellite observations as additional constraint in a joint CO_2-CO inversion. CO is measured from space with high precision, is strongly correlated with CO_2, and is more sensitive than CO_2 to CTM transport errors on synoptic and smaller scales. Exploiting this constraint requires statistics for the CTM transport error correlation between CO_2 and CO, which is significantly different from the correlation between the concentrations themselves. We estimate the error correlation globally and for different seasons by a paired-model method (comparing GEOS-Chem CTM simulations of CO_2 and CO columns using different assimilated meteorological data sets for the same meteorological year) and a paired-forecast method (comparing 48- vs. 24-h GEOS-5 CTM forecasts of CO_2 and CO columns for the same forecast time). We find strong error correlations (r^2>0.5) between CO_2 and CO columns over much of the extra-tropical Northern Hemisphere throughout the year, and strong consistency between different methods to estimate the error correlation. Application of the averaging kernels used in the retrieval for thermal IR CO measurements weakens the correlation coefficients by 15% on average (mostly due to variability in the averaging kernels) but preserves the large-scale correlation structure. We present a simple inverse modeling application to demonstrate that CO_2-CO error correlations can indeed significantly reduce uncertainty on surface carbon fluxes in a joint CO_2-CO inversion vs. a CO_2-only inversion.

Correspondence to: H. Wang
(hwang@cfa.harvard.edu)

1 Introduction

The joint Japan Aerospace Exploration Agency (JAXA), National Institute of Environmental Studies (NIES) and Ministry of the Environment (MOE) Greenhouse gases Observing SATellite (GOSAT or "Ibuki") (http://www.jaxa.jp/projects/sat/gosat/index_e.html), launched in January 2009, is expected to greatly improve our knowledge of regional CO_2 sources and sinks by providing global measurements of CO_2 dry column mixing ratios (X_{CO_2}). It detects CO_2 by solar backscatter in the 1.61 and 2.06 μm bands, together with O_2 in the 0.76 μm band, resulting in X_{CO_2} measurements with near-uniform sensitivity down to the surface. The National Aeronautics and Space Administration (NASA) Orbiting Carbon Observatory (OCO) was designed to provide global X_{CO_2} data with 0.3% (about 1 ppm) precision using the same channels (Crisp et al., 2004; Miller et al., 2007). Unfortunately, the February 2009 launch of OCO failed to reach orbit. Satellite observations of CO_2 from space are also available in the thermal IR from the AIRS (Crevoisier et al., 2003; Chahine et al., 2005, 2008; Tiwari et al., 2006; Maddy et al., 2008; Stow and Hannon, 2008), TES (Kulawik et al.,

2009), and IASI (Crevoisier et al., 2009; Clerbaux et al., 2009) instruments. These latter observations are most sensitive in the mid-troposphere. The SCIAMACHY instrument measures CO_2 using UV-vis-Near IR spectroscopy, which is sensitive in the mid-to-lower troposphere, but is presently limited to retrievals over land (Buchwitz et al., 2005a, b).

Successful exploitation of satellite CO_2 data to constrain carbon fluxes requires advanced inverse models because of the large volume of data. A number of studies have applied variational data assimilation (4D-Var) (Rodenbeck et al., 2003; Baker et al., 2006a, 2008; Chevallier et al., 2007; Engelen et al., 2009) and ensemble filtering methods (Peters, et al., 2005; Zupanski, et al., 2007; Lokupitiya et al., 2008; Feng et al., 2009; Engelen et al., 2009) for CO_2 flux inversions. The inverse model optimizes fluxes so that the mismatch between observations and the values simulated by a forward chemical transport model (CTM) are minimized under the constraint of a priori knowledge. The CTM solves the 3-D continuity equation for CO_2 concentrations using assimilated meteorological data for the observation period. Transport error in the CTM is an important factor limiting the quality of CO_2 surface flux inversions (Gurney et al., 2002, 2003, 2004; Peylin et al., 2002; Patra et al., 2006; Baker et al., 2006b, 2008).

One approach to improve the inverse CO_2 flux estimate is through the additional constraint offered by CO_2-CO error correlation in a joint CO_2-CO inversion (Palmer et al., 2006). CO is emitted by incomplete combustion and removed from the atmosphere by oxidation by the OH radical with a lifetime of two months. Several satellite instruments (MOPITT, AIRS, SCIAMACHY, TES, IASI) provide high-quality data for CO and global coverage (McMillan et al., 2005; Bowman et al., 2006; Dils et al., 2006; Calbet et al., 2006; Emmons et al., 2009). A number of studies have used satellite CO observations in inverse model analyses of CO sources (e.g., Heald et al., 2004; Arellano et al., 2004, 2006; Pfister et al., 2005; Stavrakou and Muller, 2006; Kopacz et al., 2009). CO has stronger gradients than CO_2 on account of its shorter lifetime and hence it has greater sensitivity to model transport errors on synoptic and smaller scales, as can be inferred from simple flux-gradient reasoning. If model transport errors for CO_2 and CO are correlated, then CO has the potential to provide additional information to improve inverse CO_2 flux estimates (Palmer et al., 2006). Strong correlations between CO_2 and CO concentrations are consistently seen in atmospheric observations at the surface (Potosnak et al., 1999; Gamnitzer et al., 2006) and from aircraft (Conway et al., 1993; Sawa et al., 2004; Schmitgen et al., 2004; Suntharalingam et al., 2004; Takegawa et al., 2004; Palmer et al., 2006). These correlations result from common source/sink regions, common large-scale latitudinal gradients, and common transport. For the same reasons, transport errors are expected to be correlated as well.

Palmer et al. (2006) previously conducted a joint CO_2-CO flux inversion using CO_2 and CO measurements in Asian outflow from the TRACE-P aircraft campaign over the western Pacific in March–April 2001. Observed CO_2 and CO concentrations showed correlation coefficients higher than 0.7 throughout the troposphere with distinct CO_2/CO slopes depending on air mass origin (Suntharalingam et al., 2004). Palmer et al. (2006) found that exploiting this correlation in a joint CO_2-CO flux inversion improved Asian CO_2 flux estimates significantly relative to a CO_2-only inversion. They assumed that the model transport error correlation between CO_2 and CO would be identical to the observed correlation of concentrations, but as shown below this is not a good assumption in general.

Our aim in this paper is to develop an understanding of CO_2-CO model transport error correlations as relevant to inversion of carbon fluxes from satellite observations. We present different methods for estimating the model error correlation and show that there is consistency and robustness across them. We examine the variability of the error correlation geographically, seasonally, and for satellite observations with different averaging kernels. We illustrate through a simple example how the error correlation can improve constraints on carbon fluxes.

2 Exploiting the CO_2-CO error correlation in CO_2 flux inversions

Consider the Bayesian inversion problem of constraining carbon fluxes from satellite measurements of the column mixing ratio X_{CO_2}. We follow the notation of Rodgers (2000). An ensemble of X_{CO_2} observations ($\boldsymbol{y}$, the observation vector) is used to optimize an ensemble of CO_2 surface fluxes ($\boldsymbol{x}$, the state vector) subject to prior knowledge of the fluxes (best estimate $\boldsymbol{x}_a$). The state vector is related to the observation vector $\boldsymbol{y}$ through the CTM forward model:

$$\boldsymbol{y} = F(\boldsymbol{x}) + \boldsymbol{\varepsilon} \tag{1}$$

where $\boldsymbol{\varepsilon}$ is the observational error, described in more detail below. The inverse model minimizes a cost function $J(\boldsymbol{x})$ which is the least-squares sum of the observational error weighted by the observational error covariance matrix ($\boldsymbol{S} = E(\boldsymbol{\varepsilon}\varepsilon^T)$, where E denotes the expected value operator) and the a priori error ($\boldsymbol{\varepsilon}_a = \boldsymbol{x} - x_a$) weighted by the a priori error covariance matrix ($\boldsymbol{S}_a = E(\boldsymbol{\varepsilon}_a\boldsymbol{\varepsilon}_a^T)$) (Rodgers, 2000):

$$J(\boldsymbol{x}) = \tag{2}$$
$$(\boldsymbol{y} - F(\boldsymbol{x}))^T \boldsymbol{S}^{-1}(y - F(\boldsymbol{x})) + (x - x_a)^T \boldsymbol{S}_a^{-1}(\boldsymbol{x} - x_a)$$

The a priori error describes the inaccuracy of the prior knowledge of surface fluxes. The observational error describes the inability of the forward model to match observations perfectly even if it used the true value ($\boldsymbol{x}$) of the state

vector as input. It includes contributions from instrument error ($\boldsymbol{\varepsilon}_{\mathrm{I}}$), representation error ($\boldsymbol{\varepsilon}_{\mathrm{R}}$), and forward model error ($\boldsymbol{\varepsilon}_{\mathrm{M}}$) (Heald et al., 2004; Engelen et al., 2002, 2006):

$$\boldsymbol{\varepsilon} = \varepsilon_{\mathrm{I}} + \varepsilon_{\mathrm{R}} + \varepsilon_{\mathrm{M}} \quad (3)$$

Components of the observational errors are not strictly independent. We will simplify here by ignoring their covariance. The error variances add quadratically (if the errors are independent). The instrument error includes measurement noise and retrieval error (Engelen et al., 2002, 2006). Smoothing error introduced by the averaging kernels of the satellite instrument is a source of retrieval error, but can be canceled by smoothing the CTM profiles with the same averaging kernels (Jones et al., 2003; Heald et al., 2004). Forward model error is the dominant source of observational error for CO observations from space (Heald et al., 2004) and may be dominant for CO_2 observations depending on data quality and averaging strategy (Baker et al., 2008).

The diagonal elements of the observational error covariance matrix $\boldsymbol{S}$ are the variances of observational errors for the individual components of $\boldsymbol{y}$. The off-diagonal elements are the corresponding observational error covariances, and can be obtained by scaling the error correlation coefficients with the corresponding square roots of error variances. One way to estimate the observational error variance is by the Relative Residual Error (RRE) method (Palmer et al., 2003; Heald et al., 2004). In this method, a forward model simulation using a priori fluxes ($\boldsymbol{K}x_a$) is conducted and results compared to observation time series for individual domains (such as model grid squares). The mean differences for the time series (model bias) are assumed to be due to error in the a priori fluxes. The residual differences are taken to represent the observational error.

In a joint CO_2-CO inversion, the observational vector ($\boldsymbol{y}$) consists of the CO_2 and CO observations, and the state vector ($\boldsymbol{x}$) consists of CO_2 surface fluxes and CO sources. Coupling between the CO_2 and CO inversions occurs through the corresponding off-diagonal elements of the error covariance matrices. The observational error covariance matrix now takes the form (4), where $\boldsymbol{S}_{\mathrm{CO_2}}$ and $\boldsymbol{S}_{\mathrm{CO}}$ are the error covariance matrices for the single-species inversions:

$$\boldsymbol{S} = \begin{pmatrix} \boldsymbol{S}_{\mathrm{CO_2}} & E(\boldsymbol{\varepsilon}_{\mathrm{CO_2}}\boldsymbol{\varepsilon}_{\mathrm{CO}}^T) \\ E(\boldsymbol{\varepsilon}_{\mathrm{CO}}\boldsymbol{\varepsilon}_{\mathrm{CO_2}}^T) & \boldsymbol{S}_{\mathrm{CO}} \end{pmatrix} \quad (4)$$

Since the instrument error for CO_2 and CO can be assumed independent, and the representation error can be assumed small (Heald et al., 2004), the observational error covariance between CO_2 and CO only comes from the model transport error. The CO_2-CO error covariance terms can be derived from the model error correlation coefficients by scaling by the square roots of model error variances of CO and CO_2. Although the model error variances obviously depend on the model, the correlation structure is more general as shown in Sect. 4.

In addition to observational error covariance, there could also be error correlation in the a priori emissions of CO_2 and CO due to the common combustion source. However, as shown by Palmer et al. (2006), this correlation is in fact very weak because the error in a priori CO emissions is mainly contributed by the emission factor (emission per unit fuel) rather than the activity rate (amount of fuel burned). A possible exception is biomass burning if uncertainty in activity rate exceeds a factor of two (Palmer et al., 2006). Palmer et al. (2006) found that this a priori error correlation was not useful in their inversion and we do not discuss it further here.

3 Estimating the CO_2-CO error correlation

We use two independent methods, which we call the paired-model and paired-forecast methods, to estimate the CO_2-CO model error correlation (r_M) and its geographical and seasonal distribution. In the paired-model method, we conduct otherwise identical CTM simulations of CO_2 and CO using different assimilated meteorological data sets for the same meteorological year. In the paired-forecast method, we compare 48-h vs. 24-h chemical forecasts of CO_2 and CO. The latter method has been used extensively for meteorological data assimilation and is often called the NMC method (Parish and Derber, 1992).

In both methods, each pair produces global 3-D concentration fields of CO_2 and CO for the same times that differ because of model transport error. A time series of model output for a given gridbox thus generates time series of concentration differences ΔCO_2 and ΔCO for the pair. We correlate the time series of ΔCO_2 vs. ΔCO for individual model grid boxes and individual months to estimate the corresponding CO_2-CO transport error correlation coefficients (r_M). The estimates may differ depending on the method and the data sets used, but by comparing the estimates obtained in different ways we can assess their robustness. The concentration fields are sampled as columns for the satellite overpass times and with or without instrument averaging kernels. Figure 1 shows typical averaging kernels for CO_2 from OCO (values for GOSAT are similar), CO from SCIAMACHY, and CO from AIRS. GOSAT, OCO and SCIAMACHY measure by solar backscatter in the near-IR and thus have near-unit sensitivity through the bulk of the atmosphere (i.e., nearly flat averaging kernels). AIRS, MOPITT, and TES measure in the thermal IR and have maximum sensitivity in the mid-troposphere. Infrared instruments can observe on both the night side and the day side of the orbit. On the dayside, all instruments observe at near 13:30 local time ("A-Train" constellation of satellites on the same orbit track) except for GOSAT (13:00), MOPITT (10:30) and SCIAMACHY (10:00).

For the paired-model method, we perform global simulations of CO_2 and CO using the GEOS-Chem CTM (v8-01-01, http://www-as.harvard.edu/chemistry/trop/geos) driven

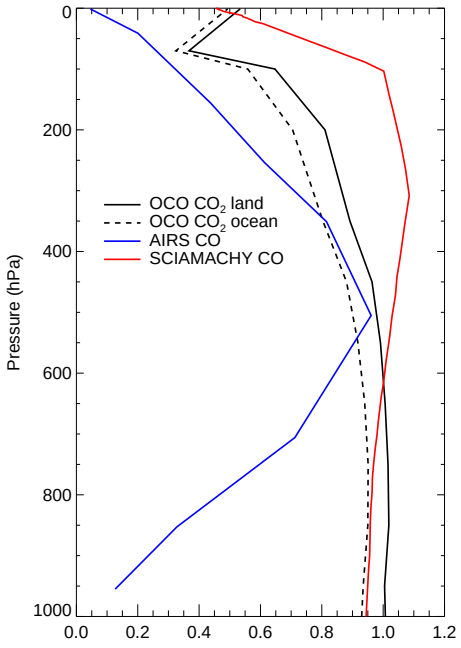

Fig. 1. Typical column averaging kernels for OCO retrieving CO_2 and for SCIAMACHY and AIRS retrieving CO. OCO kernels are for conifer and ocean surfaces with solar zenith angle of 20° and optical depth of 0.005 (Bosch et al., 2008). The AIRS kernel is for a clear-sky ocean scene at 2.2° N and 156.9° W on 1 August 2006 (http://disc.sci.gsfc.nasa.gov/AIRS). The SCIAMACHY kernel is for a solar zenith angle of 20° (Buchwitz et al., 2004).

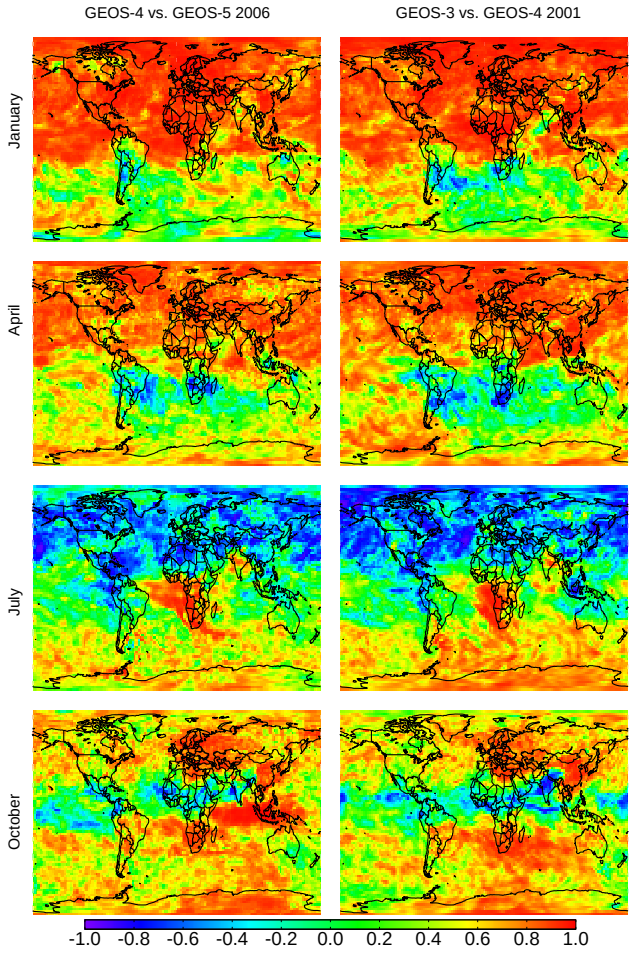

Fig. 2. Model error correlation coefficients between column CO_2 and column CO in different seasons calculated with the paired model method for GEOS-5 vs. GEOS-4 (2006) and GEOS-4 vs. GEOS-3 (2001) at 2°×2.5° resolution. Both CO_2 and CO columns were sampled at 13:30 local time. No averaging kernels were applied.

by the same sources and sinks but different generations of Goddard Earth Observing System (GEOS) assimilated meteorological data produced by the NASA Global Modeling and Assimilation Office (GMAO). We compare simulations conducted with GEOS-5 vs. GEOS-4 for 2006, and GEOS-4 vs. GEOS-3 for 2001. GEOS-3, GEOS-4, and GEOS-5 differ in the underlying general circulation model, the methodology for data assimilation, and the data assimilated (Bloom et al., 2005; Rienecker et al., 2008; Ott et al., 2009). All GEOS data sets are 6-hourly (3-hourly for mixing depth and surface variables) and are regridded to 2°×2.5° horizontal resolution for input to GEOS-Chem. The GEOS-Chem CO_2 and CO simulations have been documented previously including extensive comparisons to observations (e.g., Suntharalingam et al., 2004; Duncan et al., 2007). Anthropogenic CO_2 emissions are from Andres et al. (1996). Anthropogenic CO emissions are a combination of currently available inventories as used in Kopacz et al. (2009). Biomass burning emissions for both CO_2 and CO are from the monthly Global Fire Emission Database version 2 (GFED2) inventory for the simulation year (van der Werf, 2006). Biofuel emissions of CO_2 and CO are from Yevich and Logan (2003). All CO simulations use the same monthly 3-D OH concentration fields archived from a GEOS-Chem full-chemistry simulation (Fiore et al. 2003). Exchange of CO_2 with the terrestrial biosphere follows the CASA balanced biosphere model with prescribed diurnal cycle (Randerson et al., 1997; Olsen and Randerson, 2004). Exchange of CO_2 with the ocean follows Takahashi et al. (1997).

For the paired forecast method, we use GEOS-5 global chemical forecasts of CO and CO_2 (1/2°×2/3° horizontal resolution) for July 2008 generated by GMAO in support of the ARCTAS aircraft campaign (Jacob et al., 2009). These chemical forecasts were not custom designed for this paper. The CO simulation uses the same sources and OH fields as GEOS-Chem. The CO_2 simulation differs in using daily averaged biospheric fluxes from CASA and no biomass burning. The 48-h and 24-h forecasts were sampled at 13:30 GMT.

4 CO_2-CO error correlation patterns

Figure 2 shows the global and seasonal patterns of the model error correlation between column CO_2 and column CO calculated with the paired-model method for GEOS-4 vs. GEOS-5 (2006) and GEOS-3 vs. GEOS-4 (2001). Both CO_2 and CO are sampled at 13:30 local time, corresponding to the A-Train overpass. Results are for actual columns (no averaging kernels) and would also apply to flat averaging kernels as obtained from the near-IR GOSAT and SCIAMACHY sensors (Fig. 1).

We find in Fig. 2 strong positive correlations ($r_M > 0.7$) prevailing during the non-growing season and in biomass burning regions. In January, 92%, 80% and 45% of the area north of 30° N has $r_M > 0.7$, 0.8, and 0.9, respectively. Similarly, strong negative correlations exist in the growing season in the absence of biomass burning. In July, 26%, 11%, and 3% of the area north of 30° N has $r_M < -0.6, -0.7$, and -0.8, respectively. Due to the magnitude and variability of the CASA balanced biospheric flux, the correlations are stronger and more coherent in winter than in summer. Error correlations extend far downwind of biomass burning and fossil fuel regions and over the scale of the Northern Hemisphere. Regions of strong model error correlations include but are not limited to regions of strong model error variances. Inverse model studies of CO_2 fluxes have pointed to model transport errors in northern extra-tropical land areas as a major limiting factor in flux optimization (Gurney et al., 2002, 2003, 2004; Baker et al., 2006). The strong CO_2-CO error correlations in that region offer promise for improvements through a joint CO_2-CO inversion.

We also find in Fig. 2 that error correlation patterns are very similar for the GEOS-4/GEOS-5 and GEOS-3/GEOS-4 pairs. The robustness of error correlation patterns indicates that the directions of the general gradients of column CO and CO_2 are similar between the two sets of models. Stronger positive correlation over Indonesia and the Indian Ocean in October for the GEOS-4/GEOS-5 pair can be explained by stronger biomass burning in Indonesia in 2006 (Logan et al., 2008). We find that correlation magnitudes and patterns are insensitive to time of day (not shown), even though the CO_2 surface flux changes sign between day and night during the growing season. This is consistent with observations by Washenfelder et al. (2006) that CO_2 columns (as opposed to surface concentrations) show little diurnal variability.

Figure 3 shows the model error correlations obtained from the paired-forecast method for July 2008. As in Fig. 2, no averaging kernels are applied. Despite the differences in meteorology, emissions, sampling time, and method (Sect. 3), the large scale model error correlations are very similar to those in Fig. 2. The error structure is finer because of the higher spatial resolution (1/2°×2/3° vs. 2°×2.5°).

Figure 4 shows the error correlation results including averaging kernels for OCO CO_2 and AIRS CO, as obtained by the paired-model method for January and July 2006. For OCO

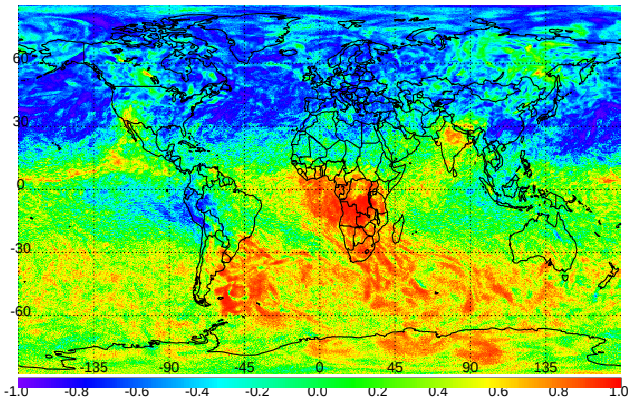

Fig. 3. Model error correlation coefficients between CO_2 and CO columns calculated with the paired-forecast method for July 2008 at 1/2°×2/3° resolution. No averaging kernels were applied. Results can be compared to the July panels of Fig. 2.

we use fixed land and ocean averaging kernels taken from Fig. 1; these do not significantly modify the CO_2 columns. Similar averaging kernels apply for GOSAT. For AIRS, we used the averaging kernels for each CO retrieval (AIRS data version 5, http://disc.sci.gsfc.nasa.gov/AIRS; McMillan et al., 2005), and averaged the resulting CO columns over the 2°×2.5° model grid. Application of AIRS averaging kernels degrades the error correlation because the CO_2 and CO columns are now observed with different and variable vertical weighting factors. Yet we find that the large-scale correlation structures are preserved (Fig. 4) with the correlation coefficients reduced on average by 15% (of which 9% is due to averaging kernel variation) relative to the results of Fig. 2.

In their previous joint CO_2-CO inverse analysis using TRACE-P aircraft data, Palmer et al. (2006) assumed that the CO_2-CO observational error correlation was the same as the correlation of concentrations. If this assumption was approximately correct it would greatly facilitate the generation of error correlation statistics. We examine its validity in Fig. 5 by showing the correlations between column CO_2 and column CO (without averaging kernels) simulated by GEOS-Chem for 2006. These can be compared to the error correlations shown in the left panels of Fig. 2. We find the same general patterns of strong positive correlations in combustion source regions, and strong negative correlations in regions of photosynthesis activity. But there are also large differences, particularly in the transition seasons (e.g., April). For the Palmer et al. (2006) conditions of Asian outflow over the NW Pacific in April, we find that the transport errors are much more strongly correlated than the columns themselves, which would increase the utility of the joint CO_2-CO inversion for constraining carbon fluxes. Overall, the differences between Fig. 2 and 5 are sufficiently large and complex that correlation of concentrations should not be used as error correlations in general.

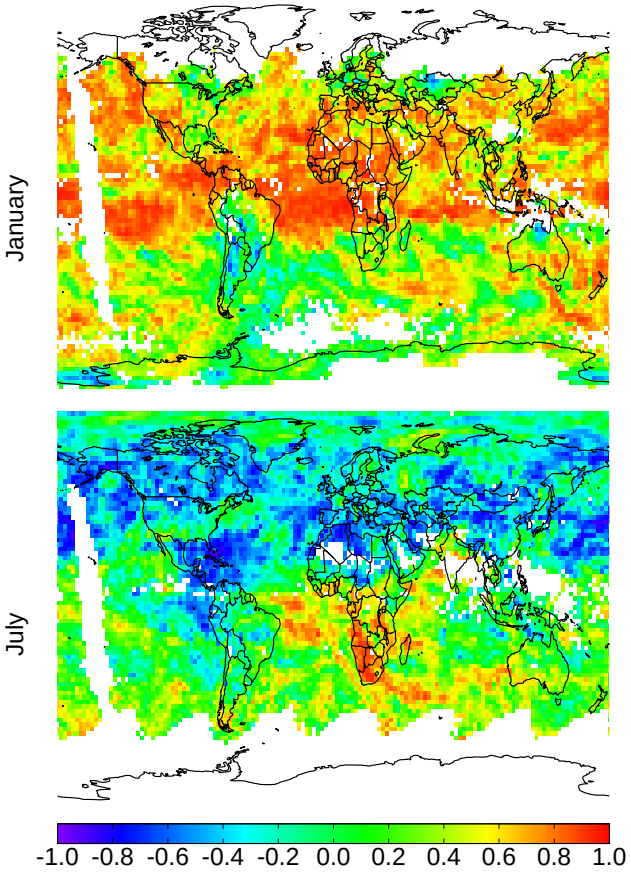

Fig. 4. CO_2-CO model error correlation coefficients between column CO_2 sampled with the land and ocean OCO averaging kernels of Fig. 1 and column CO sampled with actual AIRS averaging kernels associated with each scene. CO_2 and CO are sampled at 13:30 local time for January and July 2006 and error correlations are calculated by the paired-model (GEOS-5 vs. GEOS-4) method. Blank areas correspond to grid squares that had fewer than 21 AIRS observations for the month.

5 Demonstration of error reduction in a CO_2 flux inversion

We demonstrate the benefit of using CO_2-CO model error correlations in CO_2 flux inversions with a simple example. Pseudo data of column CO_2 and column CO with OCO-like averaging kernels (Fig. 1, OCO-land) were generated along A-train orbits using $2^\circ \times 2.5^\circ$ GEOS-Chem CO and CO_2 simulations driven by GEOS-4 meteorology. Model error variances and correlation derived from the paired model method were used to specify the observational error covariance matrix **S**. Since OCO averaging kernels essentially show uniform vertical sensitivity, we used the GEOS-5 vs. GEOS-4 correlation map without averaging kernels (Fig. 2). We assumed that the forward model error is the only source of observational error ($\varepsilon = \varepsilon_M$), and ignored spatial and temporal error correlations.

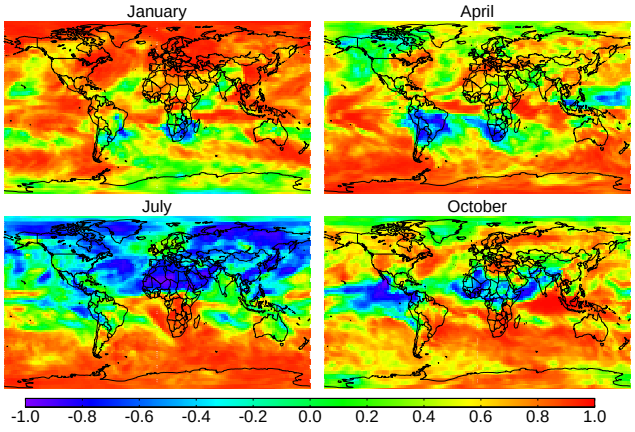

Fig. 5. Correlation coefficients between column CO_2 and column CO simulated by GEOS-Chem with GEOS-4 meteorology for 2006 at $2^\circ \times 2.5^\circ$ resolution. Both CO_2 and CO are sampled at 13:30 local time. No averaging kernels are applied.

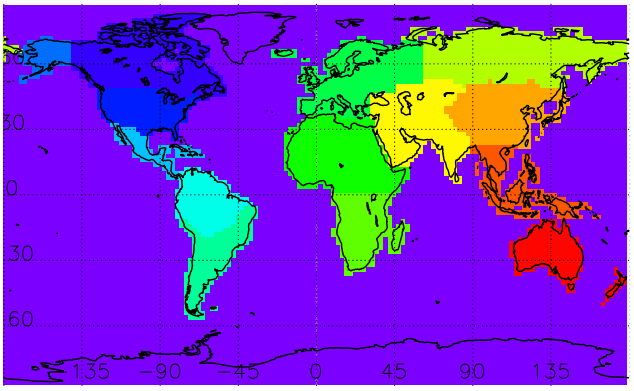

Fig. 6. The 14 land regions and rest of the world (ROW) used in the inversion example, from Nassar et al. (2009).

We performed an analytical Bayesian inversion for 14 land regions and the rest of the world (ROW) (Fig. 6) [Nassar et al., 2009] for the first two weeks of January 2006 and of July 2005. The Jacobian matrix $\mathbf{K} = \nabla_x F = \partial y / \partial x$ was constructed using a total of 45 tagged tracers. Each land region had one tracer for CO combustion, one for CO_2 combustion, and one for CO_2 biospheric exchange. In addition, there was one CO tracer and one CO_2 tracer for ROW and one CO tracer for chemical production from methane and biogenic volatile organic compounds. The a priori error covariance matrix was assumed diagonal, with 50% uncertainty for CO, 25% for combustion CO_2, 80% for biosphere CO_2 and 30% for ROW. We also performed a control CO_2-only inversion.

One way to diagnose the benefit of a CO_2-CO joint inversion relative to a CO_2-only inversion is examining the decrease in the a posteriori flux errors (Palmer et al., 2006). The a posteriori error covariance matrix $\hat{\mathbf{S}}$ is given by (Rodgers, 2000):

$$\hat{\mathbf{S}} = (\boldsymbol{K}^T \boldsymbol{S}^{-1} \boldsymbol{K} + \boldsymbol{S}_{\boldsymbol{a}}^{-1})^{-1} \quad (5)$$

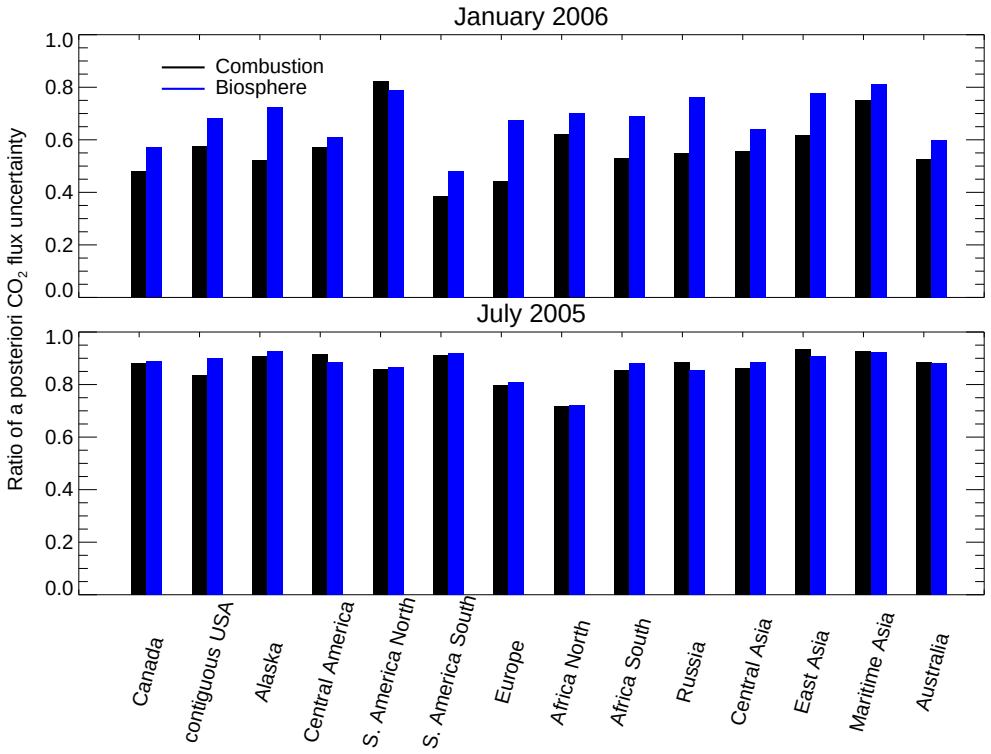

Fig. 7. Ratio of a posteriori CO_2 surface flux error between a joint CO_2-CO inversion and a CO_2-only inversion for the different regions in Fig. 6. The errors are measured as the square roots of the diagonal terms of the a posteriori error covariance matrix $\hat{\boldsymbol{S}}$. The inversions used 14 days of pseudo satellite data sampled along the A-train orbit in January 2006 (top) and July 2005 (bottom).

The a posteriori errors are the square roots of the diagonal terms of $\hat{\mathbf{S}}$. Figure 7 shows the ratios of a posteriori CO_2 flux errors between the CO_2-CO and CO_2-only inversion. In January, when strong positive model error correlations prevail in the Northern Hemisphere, a posteriori CO_2 combustion and biosphere flux uncertainties from the CO_2-CO inversion are 39–82% of those in the uncorrelated inversion, with a median of 56% for combustion sources and 69% for biosphere fluxes. In July, they typically decrease by 10–30% relative to the CO_2-only inversion. Larger improvements in January compared to July are due to generally larger absolute values of correlation coefficients and greater spatial coherence. Differences in improvement between source regions in Fig. 7 generally reflect differences in the strength of the correlation in Fig. 2. The present example indicates significant promise. Our example involves several simplifications such as neglecting instrument and representation errors, neglecting spatial and temporal correlations, and using the same model for both pseudo data and inversion. These simplifications may influence the benefits of the joint CO_2-CO inversion (Chevallier, 2007). A more extensive study will be needed to better understand their effects.

6 Conclusions

We explored the potential of using CO_2-CO transport error correlations to improve inversions of CO_2 surface fluxes from satellite observations of CO_2 columns. CO columns can be measured from space with high relative precision. Because of its relatively short lifetime, CO is more sensitive than CO_2 to model transport errors on synoptic and smaller scales. A joint CO_2-CO inversion including model transport error correlation could improve the inversion of CO_2 surface fluxes relative to a CO_2-only inversion. In this paper we showed how the CO_2-CO error correlation structure can be determined robustly on a global scale, and we presented an illustrative example to demonstrate its value for CO_2 flux inversions.

We used two independent methods to characterize the model transport error correlation for CO_2 and CO columns as measured from space. The first is a paired-model method in which we conducted CTM simulations of CO_2 and CO with the same sources and sinks for the same meteorological year but different assimilated meteorological data sets. We applied this method to GEOS-5 vs. GEOS-4 data sets for 2006 and to GEOS-4 vs. GEOS-3 data sets for 2001. The second is a paired-forecast method (often called the NMC method) in which we compared 48-h vs. 24-h CTM forecasts of CO_2

and CO for the same forecast times. We find that these different methods and data sets yield very similar large scale error correlation patterns. Strong positive error correlations are found over much of the Northern Hemisphere during the non-growing season, and over biomass burning regions of the tropics extending to the oceans far downwind. Strong negative error correlations are found over much of the Northern Hemisphere during the growing season. The correlations are largely insensitive to the time of day of the observations.

Satellite measurements by solar backscatter in the near-IR (OCO and GOSAT for CO_2, SCIAMACHY for CO) have vertically uniform sensitivities, but thermal-IR instruments (MOPITT, AIRS, TES, IASI) have greatest sensitivity in the mid-troposphere. We therefore examined the model error correlation of CO_2 with CO including variable AIRS averaging kernels for individual scenes as observed in 2006. We find that the CO_2-CO error correlation coefficients decrease by 15%, mostly due to variations in averaging kernels, but the large-scale correlation structure is preserved.

We examined whether simple correlation of concentrations could offer a suitable approximation to the error correlation since it is much easier to derive and can be constrained by observations. We find that the general patterns are often similar between the two but there are also sufficiently large differences to make the approximation inadequate.

We illustrated the potential of exploiting CO_2-CO error correlations in a joint CO_2-CO flux inversion with a simple example based on 14 days of pseudo satellite observations. We find that a posteriori CO_2 flux uncertainties are substantially reduced, implying significant improvement in the CO_2 flux inversion. Inversions using actual satellite observations are subject to measurement noise and model biases that complicate greatly the interpretation of results relative to our idealized example. Further work will be needed to demonstrate the value of CO_2-CO error correlations as constraints on CO_2 fluxes in real world applications.

Acknowledgements. Work at Harvard was funded by the NASA Atmospheric Composition Modeling and Analysis Program. Work at University of Toronto was funded by the Natural Sciences and Engineering Research Council of Canada. We thank Hartmut Bösch at University of Leicester for providing OCO averaging kernels. We thank Jean-Daniel Paris at and two anonymous reviewers for providing thoughtful comments of our paper.

Edited by: I. Aben

References

Andres, R. J., Marland, G., Fung, I., and Matthews, E.: A 1 degree $\times$1 degree distribution of carbon dioxide emissions from fossil fuel consumption and cement manufacture, 1950-1990. Global Biogeochem. Cy., 10, 3, 419–429, 1996.

Arellano, A. F., Kasibhatla, P. S., Giglio, L., van der Werf, G. R. and Randerson, J.T.: Top-down estimates of global co sources using MOPITT measurements, Geophys. Res. Lett., 31(12), L12108, doi:10.1029/2003GL018609, 2004.

Arellano, A. F., Kasibhatla, P. S., Giglio, L., van der Werf, G. R., Randerson, J. T., and Collatz, G. J.: Time-dependent inversion estimates of global biomass-burning co emissions using measurement of pollution in the troposphere (MOPITT) measurements, J. Geophys. Res., 111, D09303, doi:10.1029/2005JD006613, 2006.

Baker, D. F., Doney, S. C., and Schimel, D. S.: Variational data assimilation for atmospheric CO_2. Tellus B, 58(5), 359–365, 2006a.

Baker, D. F., Law, R. M., Gurney, K. R., Rayner, P., Peylin, P., Denning, A. S., Bousquet, P., Bruhwiler, L., Chen, Y. H., Ciais, P., Fung, I. Y., Heimann, M., John, J., Maki, T., Maksyutov, S., Masarie, K., Prather, M., Pak, B., Taguchi, S. and Zhu Z.: Transcom 3 inversion intercomparison: Impact of transport model errors on the interannual variability of regional CO_2 fluxes, 1988–2003, Global Biogeochem. Cy., 20(1), GB1002, doi:10.1029/2004GB002439, 2006b.

Baker, D. F., Bosch, H., Doney, S. C., and Schimel, D. S.: Carbon source/sink information provided by column CO_2 measurements from the Orbiting Carbon Observatory, Atmos. Chem. Phys. Discuss., 8, 20051–20112, 2008, http://www.atmos-chem-phys-discuss.net/8/20051/2008/.

Bloom, S. da Silva, A., Dee, D., Bosilovich, M., Chern, J.-D., Pawson,S., Schubert, S., Sienkiewicz, M., Stajner, I., Tan, W.-W., and Wu, M.-L.: Documentaion and validation of the Goddard Earth Observing System (GEOS) data assimilation system – Version 4. Technical report series on Global modeling and data assimilation 104606, 26, 2005.

Bowman, K. W., Rodgers, C. D., Kulawik, S. S., Worden, J., Sarkissian, E., Osterman, G., Steck, T., Lou, M., Eldering, A., Shephard, M., Worden, H., Lampel, M., Clough, S., Brown, P., Rinsland, C., Gunson, M., and Beer, R.: Tropospheric emission spectrometer: Retrieval method and error analysis, IEEE T. Geosci. Remote, 44, 1297–1307, 2006.

Buchwitz, M., de Beek, R., Bramstedt, K., Noel, S., Bovenmann, H., and Burrows, J. P.: Global carbon monoxide from SCIAMACHY by WFM-DOS, Atmos. Chem. Phys., 4, 1954–1960, 2004.

Buchwitz, M., de Beek, R., Burrows, J. P., Bovensmann, H., Warneke, T., Notholt, J., Meirink, J. F., Goede, A. P. H., Bergamaschi, P., Körner, S., Heimann, M., and Schulz, A.: Atmospheric methane and carbon dioxide from SCIAMACHY satellite data: Initial comparison with chemistry and transport models, Atmos. Chem. Phys., 5, 941–962, 2005a.

Buchwitz, M., de Beek, R., Noël, S., Burrows, J. P., Bovensmann, H., Bremer, H., Bergamaschi, P., Körner, S., and Heimann, M.: Carbon monoxide, methane, and carbon dioxide retrieved from SCIAMACHY by WFM-DOAS: year 2003 initial data set, Atmos. Chem. Phys., 5, 3313–3329, 2005b.

Calbet, X., Schlussel, P., Hultberg, T., Phillips, P., and August, T.: Validation of the operational IASI level 2 processor using airs and ECMWF data, Atmospheric Remote Sensing, Adv. Space Res., 37(12), 2299–2305, 2006.

Chahine, M., Barnet, C., Olsen, E. T., Chen, L., and Maddy, E.: On the determination of atmospheric minor gases by the method of vanishing partial derivatives with application to CO_2. Geophys. Res. Lett., 32(22), L22803, doi:10.1029/2005GL024165, 2005.

Chahine, M. T., Chen, L., Dimotakis, P., Jiang, X., Li, Q. B., Olsen, E. T., Pagano, T., Randerson, J., and Yung, Y. L.: Satellite remote sounding of mid-tropospheric CO_2. Geophys. Res. Lett., 35(17), L17807, doi:10.1029/2008GL035022, 2008.

Chevallier, F., Breon, F. M., and Rayner, P. J.: Contribution of the orbiting carbon observatory to the estimation of CO_2 sources and sinks: Theoretical study in a variational data assimilation framework, J. Geophys. Res., 112(D9), D09307, doi:10.1029/2006JD007375, 2007.

Clerbaux, C., Boynard, A., Clarisse, L., George, M., Hadji-Lazaro, J., Herbin, H., Hurtmans, D., Pommier, M., Razavi, A., Turquety, S., Wespes, C. and Coheur, P.-F.: Monitoring of atmospheric composition using the thermal infrared IASI/MetOp sounder. Atmos. Chem. Phys. Discuss., 9, 8307–8339, 2009, http://www.atmos-chem-phys-discuss.net/9/8307/2009/.

Conway, T. J., Steele, L. P., and Novelli, P. C.: Correlations among atmospheric CO_2, CH_4 and CO in the arctic, March 1989, Atmos. Environ. A-Gen., 27, 2881–2894, 1993.

Crevoisier, C., Chedin, A., and Scott, N. A.: AIRS channel selection for CO2 and other trace-gas retrievals, Q. J. Roy. Meteor. Soc., 129, 2719–274, 2003.

Crisp, D., Atlas, R. M., Breon, F. M., Brown, L. R., Burrows, J. P., Ciais, P., Connor, B. J., Doney, S. C., Fung, I. Y., Jacob, D. J., Miller, C. E., O'Brien, D., Pawson, S., Randerson, J. T., Rayner, P., Salawitch, R. J., Sander, S. P., Sen, B., Stephens, G. L., Tans, P. P., Toon, G. C., Wennberg, P. O., Wofsy, S. C., Yung, Y. L., Kuang, Z., Chudasama, B., Sprague, G., Weiss, B., Pollock, R., Kenyon, D., and Schroll, S.: The orbiting carbon observatory (oco) mission. Trace Constitutents in the Troposphere and Lower Stratosphere, Adv. Space Res., 34(4), 700–709, 2004.

Dils, B., De Maziere, M., Muller, J. F., Blumenstock, T., Buchwitz, M., de Beek, R., Demoulin, P., Duchatelet, P., Fast, H., Frankenberg, C., Gloudemans, A., Griffith, D., Jones, N., Kerzenmacher, T., Kramer, I., Mahieu, E., Mellqvist, J., Mittermeier, R. L., Notholt, J., Rinsland, C. P., Schrijver, H., Smale, D., Strandberg, A., Straume, A. G., Stremme, W., Strong, K., Sussmann, R., Taylor, J., van den Broek, M., Velazco, V., Wagner, T., Warneke, T., Wiacek, A., and Wood, S.: Comparisons between sciamachy and ground-based FTIR data for total columns of CO, CH_4, CO_2 and N_2O, Atmos. Chem. Phys., 6, 1953–1976, 2006.

Duncan, B. N., Logan, J. A., Bey, I., Megretskaia, I. A., Yantosca, R. M., Novelli, P. C., Jones, N. B., and Rinsland, C. P.: Global budget of CO, 1988–1997: Source estimates and validation with a global model, J. Geophys. Res., 112(D22), D22301, doi:10.1029/2007JD008459, 2007.

Emmons, L. K., Edwards, D. P., Deeter, M. N., Gille, J. C., Campos, T., Nedelec, P., Novelli, P., Sachse, G.: Measurements of Pollution In The Troposphere (MOPITT) validation through 2006, Atmos. Chem.Phys., 9(5), 1795–1803, 2009.

Engelen, R. J., Denning, A. S., Gurney, K. R., and TransCom: On error estimation in atmospheric CO_2 inversions, J. Geophys. Res., 107(D22), 4635, doi:10.1029/2002JD002195, 2002.

Engelen, R. J., Denning, A. S., Gurney, K. R., Law, R. M., Rayner, P. J., Baker, D., Bousquet, P., Bruhwiler, L., Chen, Y. H., Ciais, P., Fan, S., Fung, I. Y., Gloor, M., Heimann, M., Higuchi, K., John, J., Maki, T., Maksyutov, S., Masarie, K., Peylin, P., Prather, M., Pak, B. C., Sarmiento, J., Taguchi, S., Takahashi, T., and Yuen, C. W.: On error estimation in atmospheric CO_2 inversions, J. Geophys. Res., 111(D14), D14199, 2006.

Engelen, R. J., Serrar, S., and Chevallier, F.: Four-dimensional data assimilation of atmospheric CO_2 using AIRS observations, J. Geophys. Res., 114, D03303, doi:10.1029/2008JD010739, 2009.

Feng, L., Palmer, P. I., Bosch, H., and Dance, S.: Estimating surface CO_2 fluxes from space-borne CO_2 dry air mole fraction observations using an ensemble Kalman Filter, Atmos. Chem. Phys., 9, 2619–2633, 2009, http://www.atmos-chem-phys.net/9/2619/2009/.

Fiore, A. M., Jacob, D. J., Mathhur, R., and Martin, R. V.: Application of empirical orthogonal functions to evaluate ozone simulations with regional and global models, J. Geophys. Res.-Atmos., 108(D19), doi:10.1029/2002jd003151, 2003.

Gamnitzer, U., Karstens, U., Kromer, B., Neubert, R. E. M., Meijer, H. A. J., Schroeder, H., and Levin, I.: Carbon monoxide: A quantitative tracer for fossil fuel CO_2? J. Geophys. Res., 111(D22), D22302, doi:10.1029/2005JD006966, 2006.

Gurney, K. R., Law, R. M., Denning, A. S., Rayner, P. J., Baker, D., Bousquet, P., Bruhwiler, L., Chen, Y. H., Ciais, P., Fan, S., Fung, I. Y., Gloor, M., Heimann, M., Higuchi, K., John, J., Maki, T., Maksyutov, S., Masarie, K., Peylin, P., Prather, M., Pak, B. C., Randerson, J., Sarmiento, J., Taguchi, S., Takahashi, T., and Yuen, C. W.: Towards robust regional estimates of CO_2 sources and sinks using atmospheric transport models, Nature, 415, 626–630, 2002.

Gurney, K. R., Law, R. M., Denning, A. S., Rayner, P. J., Baker, D., Bousquet, P., Bruhwiler, L., Chen, Y. H., Ciais, P., Fan, S. M., Fung, I. Y., Gloor, M., Heimann, M., Higuchi, K., John, J., Kowalczyk, E., Maki, T., Maksyutov, S., Peylin, P., Prather, M., Pak, B. C., Sarmiento, J., Taguchi, S., Takahashi, T. and Yuen, C. W.: Transcom 3 CO_2 inversion intercomparison: 1. Annual mean control results and sensitivity to transport and prior flux information, Tellus B, 55(2), 580–595, 2003.

Gurney, K. R., Law, R. M., Denning, A. S., Rayner, P. J., Pak, B. C., Baker, D., Bousquet, P., Bruhwiler, L., Chen, Y. H., Ciais, P., Fung, I. Y., Heimann, M., John, J., Maki, T., Maksyutov, S., Peylin, P., Prather, M. and Taguchi, S.: Transcom 3 inversion intercomparison: Model mean results for the estimation of seasonal carbon sources and sinks, Global Biogeochem. Cy., 18(1), GB1010, doi:10.1029/2003GB002111,2004.

Heald, C. L., Jacob, D. J., Jones, D. B. A., Palmer, P. I., Logan, J. A., Streets, D. G., Sachse, G. W., Gille, J. C., Hoffman, R. N., and Nehrkorn, T.: Comparative inverse analysis of satellite (MOPITT) and aircraft (TRACE-P) observations to estimate Asian sources of carbon monoxide, J. Geophys. Res., 109(D23), D23306, doi:10.1029/2004JD005185, 2004.

Jones, D. B. A., Bowman, K. W., Palmer, P. I., et al.: Potential of observations from the Tropospheric Emission Spectrometer to constrain continental sources of carbon monoxide, J. Geophys. Res.-Atmos., 108(D24), doi:10.1029/2003JD003702, 2003.

Kopacz, M., Jacob, D. J., Henze, D. K., Heald, C. L., Streets, D. G., and Zhang, Q.: Comparison of adjoint and analytical Bayesian inversion methods for constraining Asian sources of carbon monoxide using satellite (MOPITT) measurements of CO columns, J. Geophys. Res., 114, D04305, doi:10.1029/2007JD009264, 2009.

Kulawik, S. S., Jones, D. B. A., Nassar, R., et al.: Characterization of Tropospheric Emission Spectrometer (TES) CO_2 for carbon cycle science, Atmos. Chem. Phys., in preparation, 2009.

Logan, J. A., Megretskaia, I. A., Nassar, R., Murray, L. T., Zhang,

L., Bowman, K. W., Worden, H. M., and Luo, M.: Effects of the 2006 El Niño on tropospheric composition as revealed by data from the Tropospheric Emission Spectrometer (TES), Geophys. Res. Lett., 35, L03816, doi:10.1029/2007GL031698, 2008.

Lokupitiya, R. S., Zupanski, D., Denning, A. S., Kawa, S. R., Gurney, K. R., and Zupanski, M.: Estimation of global CO2 fluxes at regional scale using the maximum likelihood ensemble filter, J. Geophys. Res., 113(D20), D20110, doi:10.1029/2007JD009679, 2008.

Maddy, E. S., Barnet, C. D., Goldberg, M., Sweeney, C., and Liu, X.: CO_2 retrievals from the Atmospheric Infrared Sounder: Methodology and validation, J. Geophys. Res., 113, D11301, doi:10.1029/2007JD009402, 2008.

McMillan, W. W., Barnet, C., Strow, L., Chahine, M. T., McCourt, M. L., Warner, J. X., Novelli, P. C., Korontzi, S., Maddy, E. S., and Datta, S.: Daily global maps of carbon monoxide from nasa's atmospheric infrared sounder, Geophys. Res. Lett., 32(11), L11801, doi:10.1029/2004GL021821, 2005.

Miller, C. E., Crisp, D., DeCola, P. L., Olsen, S. C., Randerson, J. T., Michalak, A. M., Alkhaled, A., Rayner, P., Jacob, D. J., Suntharalingam, P., Jones, D. B. A., Denning, A. S., Nicholls, M. E., Doney, S. C., Pawson, S., Boesch, H., Connor, B. J., Fung, I. Y., O'Brien, D., Salawitch, R. J., Sander, S. P., Sen, B., Tans, P., Toon, G. C., Wennberg, P. O., Wofsy, S. C., Yung, Y. L. and Law, R.M.: Precision requirements for space-based X_{CO_2} data, J. Geophys. Res., 112(D10), D10314, doi:10.1029/2006JD007659, 2007.

Nassar, R., Jones, D. B. A., Kulawik, S. S., and Chen, J. M.: Use of surface and space-based CO_2 observations for inverse modeling of CO_2 sources and sinks. 2nd NACP All-investigators meeting, San Diego, CA, USA, 2009.

Olsen, S. C. and Randerson, J. T.: Differences between surface and column atmospheric CO_2 and implications for carbon cycle research. J. Geophys. Res., 109(D2), D02301, doi:10.1029/2003JD003968, 2004.

Ott, L. E., Bacmeister, J., Pawson, S., Pickering, K., Stenchikov, G., Suarez, M., Huntrieser, H., Loewenstein, M., Lopez, J., and Xueref-Remy, I.: Analysis of convective transport and parameter sensitivity in a single column version of the Goddard Earth Observation System, Version 5, General Circulation Model, J. Atmos. Sci., 66(3), 627–646, 2009.

Palmer, P. I., Jacob, D. J., Jones, D. B. A., Heald, C. L., Yantosca, R. M., Logan, J. A., Sachse, G. W. and Streets, D. G.: Inverting for emissions of carbon monoxide from Asia using aircraft observations over the western pacific, J. Geophys. Res., 108(D21), 8828, doi:10.1029/2003JD003397, 2003.

Palmer, P. I., Suntharalingam, P., Jones, D. B. A., Jacob, D. J., Streets, D. G., Fu, Q. Y., Vay, S. A., and Sachse, G. W.: Using CO_2: CO correlations to improve inverse analyses of carbon fluxes, J. Geophys. Res., 111 (D12), D12318, doi:10.1029/2005JD006697, 2006.

Parish, D. F. and Derber, J. C.: The National Meteorological Center's spectral statistical interpolation analysis system, Mon. Weather Rev., 120, 1747–1763, 1992.

Patra, P. K., Gurney, K. R., Denning, A. S., Maksyutov, S., Nakazawa, T., Baker, D., Bousquet, P., Bruhwiler, L., Chen, Y. H., Ciais, P., Fan, S. M., Fung, I., Gloor, M., Heimann, M., Higuchi, K., John, J., Law, R. M., Maki, T., Pak, B. C., Peylin, P., Prather, M., Rayner, P. J., Sarmiento, J., Taguchi, S., Takahashi, T., and Yuen, C. W.: Sensitivity of inverse estimation of annual mean CO_2 sources and sinks to ocean-only sites versus all-sites observational networks, Geophys. Res. Lett., 33(5), L05814, doi:10.1029/2005GL025403,2006.

Peters, W., Miller, J. B., Whitaker, J., Denning, A. S., Hirsch, A., Krol, M. C., Zupanski, D., Bruhwiler, L., and Tans, P. P.: An ensemble data assimilation system to estimate CO_2 surface fluxes from atmospheric trace gas observations, J. Geophys. Res., 110(D24), D24304, doi:10.1029/2005JD006157, 2005.

Peylin, P., Baker, D., Sarmiento, J., Ciais, P., and Bousquet, P.: Influence of transport uncertainty on annual mean and seasonal inversions of atmospheric CO_2 data, J. Geophys. Res., 107(D19), 4385, doi:10.1029/2001JD000857, 2002.

Pfister, G., Hess, P. G., Emmons, L. K., Lamarque, J. F., Wiedinmyer, C., Edwards, D. P., Petron, G., Gille, J. C., and Sachsa, G. W.:Quantifying CO emissions from the 2004 Alaska wildfires using MOPITT CO data, Geophys. Res. Lett., 32(11), L11809, doi:10.1029/2005GL022995, 2005.

Potosnak, M. J., Wofsy, S. C., Denning, A. S., Conway, T. J., Munger, J. W., and Barnes, D. H.: Influence of biotic exchange and combustion sources on atmospheric CO_2 concentrations in new england from observations at a forest flux tower, J. Geophys. Res., 104, 9561–9569, 1999.

Randerson, J. T., Thompson, M. V., Conway, T. J., Fung, I. Y., and Field, C. B.: The contribution of terrestrial sources and sinks to trends in the seasonal cycle of atmospheric carbon dioxide, Global Biogeochem. Cy. 11(4), 535–560, 1997.

Rienecker, M. M., Suarez, M. J., Todling, R., Bacmeister, J., Takacs, L., Liu, H.-C., Gu, W., Sienkiewicz, M., Koster, R. D., Gelaro, R., Stajner, I., and Nielsen, J. E.: The GEOS-5 data assimilation system – Documentation of Versions 5.0.1, 5.1.0 and 5.2.0, Technical report series on global modeling and data assimilation, 27, NASA/TM-2008-104606, Vol. 27, 2008.

Rodenbeck, C., Houweling, S., Gloor, M., and Heimann, M.: CO_2 flux history 1982-2001 inferred from atmospheric data using a global inversion of atmospheric transport, Atmos. Chem. Phys., 3, 1919–1964, 2003, http://www.atmos-chem-phys.net/3/1919/2003/.

Rodgers, C.D. : Inverse Methods for Atmospheric Sounding, World Sci., Singapore, 2000.

Sawa, Y., Matsueda, H., Makino, Y., Inoue, H. Y., Murayama, S., Hirota, M., Tsutsumi, Y., Zaizen, Y., Ikegami, M., and Okada, K.: Aircraft observation of CO_2, CO, O_3 and H_2 over the north pacific during the pace-7 campaign, Tellus B, 56, 2–20, 2004.

Schmitgen, S., Geiss, H., Ciais, P., Neininger, B., Brunet, Y., Reichstein, M., Kley, D., and Volz-Thomas, A.: Carbon dioxide uptake of a forested region in southwest france derived from airborne co2 and co measurements in a quasi-lagrangian experiment, J. Geophys. Res., 109(D14), D14302, doi:10.1029/2003JD004335, 2004.

Stavrakou, T. and Muller, J. F.: Grid-based versus big region approach for inverting CO emissions using measurement of pollution in the troposphere (MOPITT) data, J. Geophys. Res., 111(D15), D15304, doi:10.1029/2005JD006896, 2006.

Strow, L. L. and Hannon, S. E.: A 4-year zonal climatology of lower tropospheric CO_2 derived from ocean-only Atmospheric Infrared Sounder observations, 113(D18), D18302, doi:10.1029/2007JD009713, 2008.

Suntharalingam, P., Jacob, D. J., Palmer, P. I., Logan, J. A., Yan-

tosca, R. M., Xiao, Y. P., Evans, M. J., Streets, D. G., Vay, S. L., and Sachse, G. W.: Improved quantification of Chinese carbon fluxes using CO_2/CO correlations in Asian outflow, Global Biogeochem. Cy., 109(4), GB4003, doi:10.1029/2005GB002466, 2005.

Takahashi, T., Feely, R. A., Weiss, R. F., Wanninkhof, R. H., Chipman, D. W., Sutherland, S. C. and Takahashi, T. T.: Global air-sea flux of CO_2: An estimate based on measurements of sea-air pCO_2 difference, P. Natl. Acad. Sci. USA, 94(16), 8292–8299, 1997.

Takegawa, N., Kondo, Y., Koike, M., Chen, G., Machida, T., Watai, T., Blake, D. R., Streets, D. G., Woo, J. H., Carmichael, G. R., Kita, K., Miyazaki, Y., Shirai, T., Liley, J. B. and Ogawa, T.: Removal of NO_x and NO_y in Asian outflow plumes: Aircraft measurements over the western pacific in January 2002, J. Geophys. Res., 109(D23), D23S04, doi:10.1029/2004JD004866, 2004.

Tiwari, Y. K., Gloor, M., Engelen, R. J., Chevallier, F., Rodenbeck,C., Korner, S., Peylin, P., Braswell, B. H., and Heimann, M.: Comparing CO_2 retrieved from Atmosperic Infrared Sounder with model predictions: Implications for constraining surface fluxes and lower-to-upper troposphere transport, J. Geophys. Res., 111, D17106, doi:10.1029/2005JD006681, 2006.

van der Werf, G. R., Randerson, J. T., Giglio, L., Collatz, G. J., Kasibhatla, P. S., and Arellano, A. F.: Interannual variability in global biomass burning emissions from 1997 to 2004, Atmos. Chem. Phys., 6, 3423–3441, 2006.

Washenfelder, R. A., Toon, G. C., Blavier, J. F., Yang, Z., Allen, N. T., Wennberg, P. O., Vay, S. A., Matross, D. M., and Daube, B. C.: Carbon dioxide column abundances at the Wisconsin Tall Tower site, J. Geophys. Res., 111(D22), D22305, doi:10.1029/2006JD007154, 2006.

Yevich, R. and Logan, J. A.: An assessment of biofuel use and burning of agricultural waste in the developing world, Global Biogeochem. Cy., 17(4), 1095, doi:10.1029/2002GB001952, 2003.

Zupanski, D., Denning, A. S., Uliasz, M., Zupanski, M., Schuh, A. E., Rayner, P. J., Peters, W., and Corbin, K. D.: Carbon flux bias estimation employing maximum likelihood ensemble filter (MLEF), J. Geophys. Res., 112(D17), D17107, doi:10.1029/2006JD008371, 2007.